J Mater Sci (2011) 46:6408–6415
DOI 10.1007/s10853-011-5590-9

Ab initio molecular dynamics simulation of pressure-induced phase transformation in BeO

H. Y. Xiao · G. Duan · X. T. Zu · W. J. Weber

Received: 13 March 2011 / Accepted: 25 April 2011 / Published online: 5 May 2011

Abstract Ab initio molecular dynamics (MD) method has been used to study high pressure-induced phase transformation in BeO based on the local density approximation (LDA) and the generalized gradient approximation (GGA). Both methods show that the wurtzite (WZ) and zinc blende (ZB) BeO transforms to the rocksalt (RS) structure smoothly at high pressure. The transition pressures obtained from the LDA method are about 40 GPa larger than the GGA result for both WZ → RS and ZB → RS phase transformations, and the phase transformation mechanisms revealed by the LDA and GGA methods are different. For WZ → RS phase transformations both mechanisms obtained from the LDA and GGA methods are not comparable to the previous ab initio MD simulations of WZ BeO at 700 GPa based on the GGA method. It is suggested that the phase transformation mechanisms of BeO revealed by the ab initio MD simulations are affected remarkably by the exchange–correlation functional employed and the way of applying pressure.

H. Y. Xiao (✉) · G. Duan · X. T. Zu
Department of Applied Physics, University of Electronic Science and Technology of China, Chengdu 610054, People's Republic of China
e-mail: hyxiao@uestc.edu.cn

H. Y. Xiao · W. J. Weber
Department of Materials Science & Engineering, University of Tennessee, Knoxville, TN 37996, USA

W. J. Weber
Materials Science & Technology Division, Oak Ridge National Laboratory, Oak Ridge, TN 37831, USA

Introduction

Beryllium oxide (BeO) has attracted substantial attention due to its fascinating mechanical and thermal properties, such as high thermal conductivity [1], high electrical resistivity [2], high thermal stability (melting temperature $T_m = 2550°C$), high hardness [3], and radiation resistance. These properties make it useful for prospective coatings [4], nanodevices [5, 6], and applicable as principal reactor moderating material [7] and chip carrier substrate for high power applications [8]. Among the alkali earth oxides, BeO has attracted particular interest also because it is the only oxide in this family that crystallizes in hexagonal wurtzite structure at ambient conditions, whereas others occur in the cubic rocksalt structure. As a consequence, extensive experimental and theoretical studies have been performed on BeO [1–3, 7, 9–25].

The phase stability of BeO under high pressure has been a subject of several experimental and theoretical investigations. Jephcoat et al. [10] studied the Raman spectroscopy of BeO in the diamond-anvil cell and no evidence of a phase transition from the wurtzite structure was observed. Recently, Mori et al. [14] performed a high pressure X-ray diffraction experiment on BeO, and it was shown that there was no phase transition up to 126 GPa, but a new phase was observed at 137 GPa. Theoretically, significant discrepancy exists between the high pressure response behavior of BeO and the phase transformation pressure because of the various approximations and computational methods. Earlier first-principles pseudopotential calculation [17] suggested that a high pressure-induced WZ → RS phase transformation occurred at 22 GPa, while Jephcoat et al. [10] predicted a transformation pressure of 40 GPa by potential-induced-breathing method. Subsequently, it was suggested that the WZ phase of BeO first transformed to

zinc blende structure and then to RS state. The WZ → ZB and ZB → RS phase transformation have been predicted to be 74 and 137 GPa by Van Camp and Van Doren [19] employing soft nonlocal pseudopotential, 63–76 and 95 GPa by Boettger and Wills [20] using an all-electron and full-potential electronic structure calculation, and 91 and 147 GPa by Park et al. [21] using a first-principles soft nonlocal pseudopotential method within the GGA method. Recently, Cai et al. [23] studied the phase transition sequence in BeO using first-principles enthalpy calculations. Based on enthalpy calculations they suggested that WZ → ZB → RS phase transformation sequence do not occur up to 200 GPa, and around 105 GPa, the WZ BeO structure can transform to RS structure. Using the full-potential linearized-augmented plane wave method, Amrani et al. [24] predicted a similar transformation pressure of 107 GPa for WZ → RS phase transformation and a ZB → RS phase transformation at 110 GPa, in which no WZ → ZB phase transformation was predicted. It is obvious that phase stability of BeO under high pressure demands further study to resolve these discrepancies. On the other hand, Alptekin and Durandurdu [26] performed a constant pressure ab initio molecular dynamics (MD) simulation of pressure-induced phase transformation in BeO using the GGA method and the exchange–correlation functional of Perdew–Burke and Ernzerh. It was observed that WZ BeO transformed to RS phase at high pressure, passing through a fivefold coordinated hexagonal intermediate state with space group $P6_3/mmc$ and a fivefold coordinated orthorhombic intermediate state with *Cmcm* symmetry; however, the transition pressure was very high, up to 700 GPa. In our previous study on the high pressure-induced phase transition from hexagonal wurtzite to rock-salt structure in both SiC and GaN [27], we found that such high pressure could change the phase transition mechanism. It is necessary to simulate the phase stability of BeO at lower pressure to find out if the over-applied high pressure in the simulation changes the phase transformation pathway.

In this work, ab initio MD method has been employed to study the high pressure-induced phase transformation in BeO. It is observed that the WZ BeO transforms to the RS structure smoothly without passing through the ZB phase at 180 and 140 GPa for the LDA and GGA methods, respectively. The phase transformation mechanisms revealed from the simulations turn out to be dependent on the exchange–correlation functional employed, whereas the mechanisms obtained from both methods are different from the previous work reported at 700 GPa. For comparison, the phase stability of ZB BeO under high pressure is also studied. It is found that the ZB to RS structural transformation occurs at 160 GPa for the LDA method and 120 GPa for the GGA method. Discrepancy also exists in the phase transformation mechanisms obtained by the LDA and GGA methods. This study shows that the phase transformation mechanisms obtained from the ab initio MD simulations are affected by the exchange–correlation functional employed and the way of applying pressure.

Computational method

Our calculations were based on density functional theory within the framework of LDA using the Ceperley–Alder functional and GGA using Perdew–Burke–Ernzerhof functional. All the calculations were performed by SIESTA [28] code, in which a linear combination of atomic orbitals was used as the basis set. The electron–ion interactions were described by normconserving Troullier–Martins pseudopotentials [29]. The reference electronic configurations for the pesudopotentials are $2s^2 2p^0 3d^0 4f^0$ for the Be atom and $2s^2 2p^4 3d^0 4f^0$ for the O atom. The pseudopotential core radii are 2.18, 2.18, 2.47 and 2.47 Bohr for Be 2 *s*, 2*p*, 3*d*, 4*f* channels, respectively, and 1.48, 1.48, 1.48, 1.48 Bohr for O 2*s*, 2*p*, 3*d*, and 4*f* channels. The simulation cell consists of 64 atoms with periodic boundary conditions. The convergence of our calculations has been tested by the LDA method. The variation of the total energy of the WZ BeO with the mesh cutoff energy for different basis sets (single-ζ: SZ; double-ζ: DZ; double-ζ plus polarization orbitals: DZP) with a 1×1×1 k-point sampling and for different k-point sampling with a DZP basis set have been shown in Fig. 1a and b, respectively. A 2×2×2 k-point sampling in the Brillouin zone, double-ζ basis set plus polarization orbitals (DZP) and a 150 Ry cutoff for the real space mesh turn out to give good converged results. The system was first equilibrated at 300 K and zero pressure, which means that the atoms are assigned random initial velocities drawn from the Maxwell–Bolztman distribution at the temperature of 300 K. The external pressure was applied by the Parrinello and Rahman method [30] and increased at a rate of 20 GPa. The equilibration period is 2000 time steps for each increment and each time step is one femtosecond.

Results and discussion

Ab initio calculations of high pressure-induced phase transformation in BeO

Ab initio total energy calculations based on density functional theory have been used to optimize the lattice parameters of WZ, ZB, and RS BeO. The LDA method yields lattice parameters of $a_0 = 2.75$ Å, $c_0/a_0 = 1.618$ for wurtzite BeO, agreeing well with experimental values of

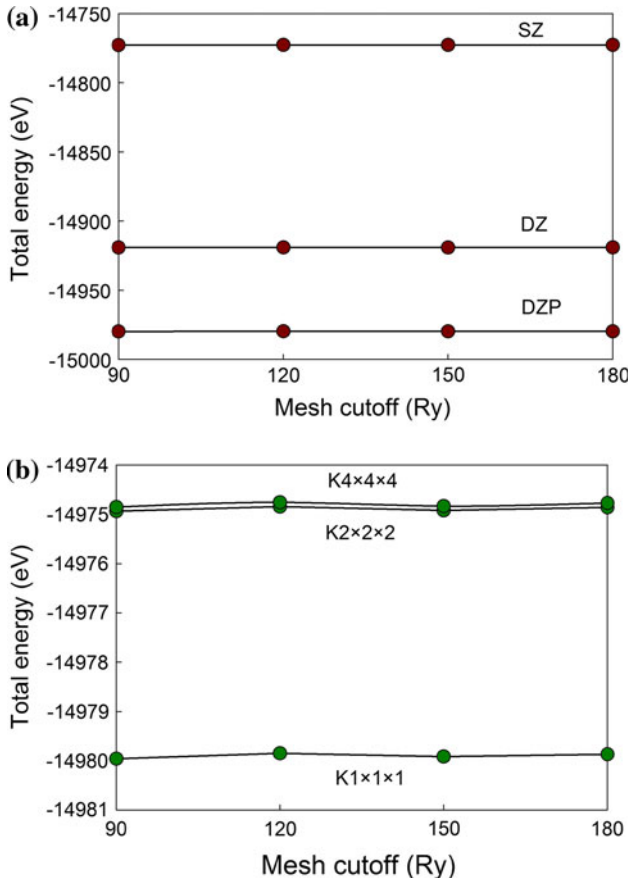

Fig. 1 Variation of the total energy of the WZ BeO with the mesh cutoff energy for **a** different basis sets with a 1×1×1 k-point sampling and **b** different k-point sampling with a DZP basis set

$a_0 = 2.693$ Å, $c_0/a_0 = 1.623$ [31]. For zinc blende BeO, the lattice constant is 3.88 Å, consistent with other theoretical value of 3.81 Å [5]. The calculated lattice constant for rocksalt BeO is 3.71 Å. For the GGA calculations, the optimized lattice parameters are $a_0 = 2.79$ Å, $c_0/a_0 = 1.615$ for wurtzite phase, $a_0 = 3.94$ Å for zinc blende structure and $a_0 = 3.71$ Å for rocksalt BeO.

To predict the phase stability of BeO, the enthalpies ($H = E + PV$) of WZ, ZB, and RS BeO from 0 to 80 GPa are calculated. These calculations were based on a simulation cell consisting of 64 atoms for each phase with a 4×4×4 k-point sampling in reciprocal space and a cutoff energy of 150 Ry for the real space mesh. Figure 2 shows the enthalpy differences between the WZ and RS BeO as a function of pressure obtained from both LDA and GGA methods. The LDA and GGA methods predict a WZ → RS Phase transformation at 34 and 26 GPa, respectively, which are significantly smaller than the experimental value of 137 GPa [31] and the theoretical value of 105 GPa reported by Cai et al. [23]. Our GGA results also differ significantly from the predicted value of 70 GPa reported by Alptekin and Durandurdu [26], and we found their

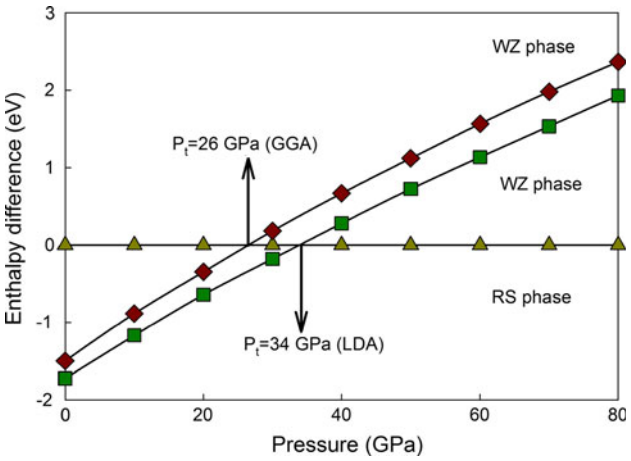

Fig. 2 The calculated enthalpy difference between WZ and RS phases as a function of pressure from both LDA and GGA methods

results can be reproduced only with the SZ basis set. ZB phase is also stable thermodynamically at ambient pressure, whereas it is always ~0.05 eV/pair higher in energy than the WZ phase during the pressure range of 0–80 GPa, and no WZ → ZB phase transformation is predicted. Our calculations also predict a ZB → RS phase transformation. The phase transformation pressure of 33 and 25 GPa by the LDA and GGA methods, respectively, are nearly the same as the results for the WZ → RS phase transformation. This is different from our previous work on GaN [27, 32], in which the WZ → RS transition pressure of 43 GPa is slightly larger than the value of 34 GPa for the ZB → RS phase transformation.

Ab initio MD simulations of WZ BeO under high pressure

In our ab initio MD simulations based on the LDA method, a pressure higher than 34 GPa is applied to accelerate the phase transition in WZ BeO. The system remains the wurtzite structure up to 160 GPa, and a phase transition from the WZ to RS structure occurs when the pressure is increased to 180 GPa, which is comparable to the experimental value of 137 GPa [31]. During the phase transformation, it is shown that WZ BeO transforms to RS structure without passing through ZB state, agreeing well with our ab initio predictions and experiments [31]. To provide a clear picture of the transformation mechanism at the microscopic level, Fig. 3 shows the variation of the simulation cell lengths with time at 180 GPa for WZ BeO. The simulation cell vectors **A**, **B**, and **C** are along the $[1\bar{2}10]$, $[10\bar{1}0]$, and [0001] directions in the original wurtzite structure, respectively. It can be seen that the phase transformation is a very fast process, and occurs within about 0.2 ps at 180 GPa. Also, the phase

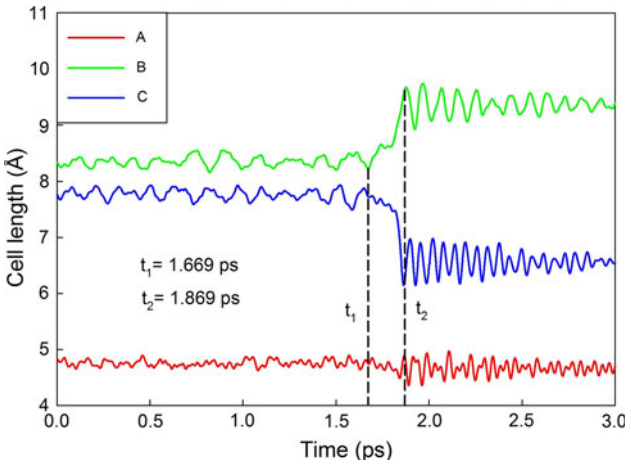

Fig. 3 Variation of the simulation cell lengths as a function of MD time step for WZ BeO at 180 GPa obtained from the LDA method

transformation proceeds very smoothly. At $t \approx 1.669$ ps, the structure starts to compress along the original wurtzite [0001] direction, and expand along the original wurtzite $[10\bar{1}0]$ direction, which is characterized by a decrease of |**C**| and an expansion of |**B**|. During the whole process, the simulation cell length |**A**| oscillates slightly with time evolution. Besides, the alpha, beta and gamma, which are angles between the **A** and **C** lattice vectors, B and C lattice vectors, and the **A** and **B** lattice vectors, respectively, oscillate marginally around 90° during the whole transition process. At $t \approx 1.869$ ps, a complete phase transformation is observed. Figure 4a illustrates the schematic view of the initial and final structures of BeO at 180 GPa. Each atom in the final phase is six-coordinated to its nearest neighboring atoms and the phase is identified as RS structure. The atomic structure and coordination of BeO before and after phase transformation are shown in Fig. 4b. Before transformation, the O_1 atom is four-coordinated to Be_2, Be_4, Be_5, and Be_6 atoms with an average bond length of 1.46 Å, and the distance from O_1 to Be_1 and Be_3 atom is 2.38 and 2.83 Å, respectively. After phase transformation the O_1 atom is coordinated to six beryllium atoms with an average bond length of 1.63 Å, and the O_1 atom is located in the same plane as Be_3, Be_4, Be_5 and Be_6 atoms, as shown in Fig. 4c. The bonding distance between Be_3 and Be_4 is 4.18 and 3.25 Å before and after transformation, respectively. For the bonding distance between Be_5 and Be_6, it is 2.4 Å before transformation and 3.25 Å after transformation. Figure 4c also shows that the atoms in the simulation cell shift toward opposite directions: $[1\bar{2}10]$ and $[\bar{1}2\bar{1}0]$, accompanied by shift in $[10\bar{1}0]$ and $[000\bar{1}]$ directions, resulting in a phase transformation to rocksalt structure.

The GGA method, on the other hand, reveals a different transformation mechanism. It is observed that the wurtzite structure remains stable up to 120 GPa, and it goes through a

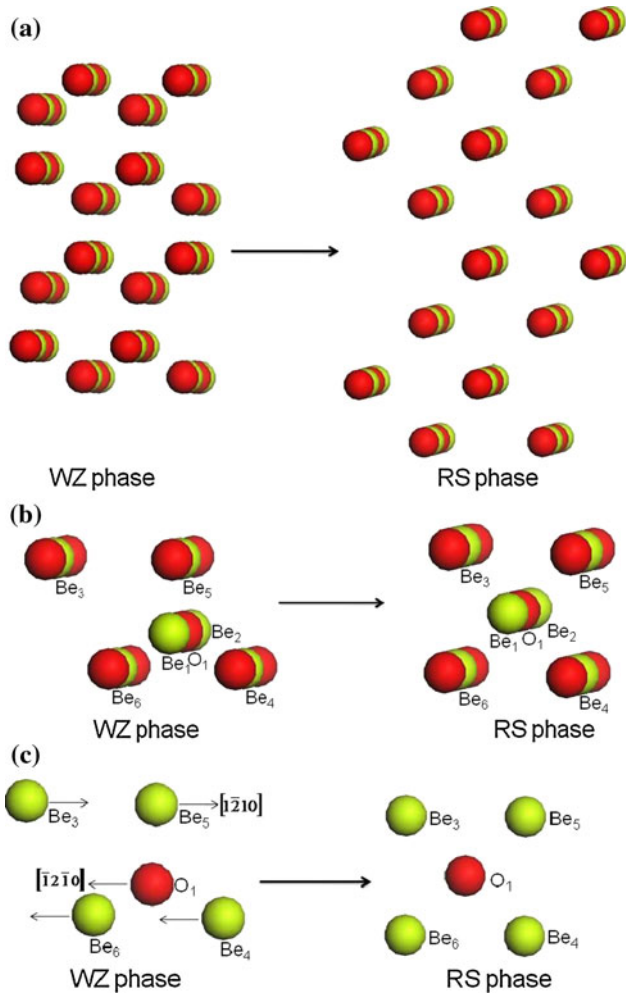

Fig. 4 Schematic view (on the (001) plane) of **a** the geometrical structure, **b** atomic coordination, **c** planar atomic structure of BeO at 180 GPa before (WZ structure) and after (RS structure) phase transformation obtained from the LDA method

phase transition to RS structure at 140 GPa. This transition pressure is in better agreement with experimental value of 137 GPa [14]. The variation of the simulation cell lengths with time at transition pressure, as presented in Fig. 5a, shows similar characters to the LDA method (see Fig. 3); however, Fig. 5b shows that the simulation angle gamma undergoes significant change during the phase transformation process, different from the case of the LDA method. The schematic views of the geometrical structure, atomic coordination and planar atomic structure of BeO at 140 GPa before and after phase transformation obtained from the GGA method are shown in Fig. 6. Accompanying the monoclinic deformation of the simulation cell, all the atoms shift in the $[\bar{1}2\bar{1}0]$ direction with different displacement. For example, the Be_3 and Be_5 atoms shown in Fig. 6c go through more considerable shift than the Be_4 and Be_6 atoms. In the meantime, atoms in the cell also shift in $[10\bar{1}0]$ and $[000\bar{1}]$ directions until the phase transformation are completed.

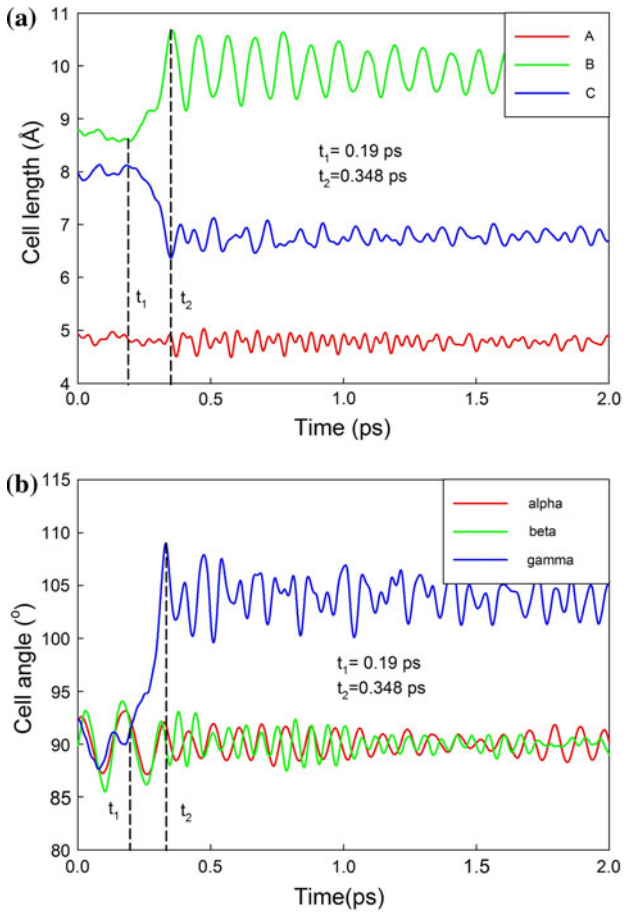

Fig. 5 Variation of the simulation cell lengths (**a**) and angles (**b**) as a function of MD time step for WZ BeO at 140 GPa obtained from the GGA method

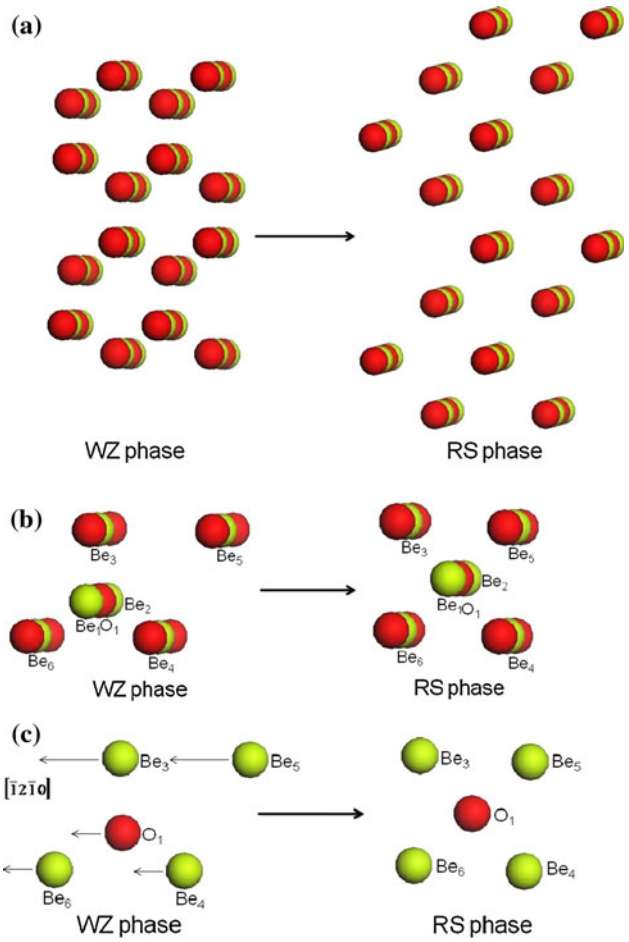

Fig. 6 Schematic view (on the (001) plane) of **a** the geometrical structure; **b** atomic coordination; **c** planar atomic structure of BeO at 140 GPa before (WZ structure) and after (RS structure) phase transformation obtained from the GGA method

In our previous work on high pressure-induced phase transformation in wurtzite GaN and SiC [27], it was shown that as the WZ structure completely transformed to the RS structure, the three simulation cell lengths became equal to each other ($|\mathbf{A}| = |\mathbf{B}| = |\mathbf{C}|$) and the three simulation angels remained to be the same as those before the phase transformation ($\alpha = \beta = \gamma = 90°$). It is obvious that the phase transformation mechanism in BeO is different from that in GaN and SiC. For the WZ → RS transformation, two representative transition models have been proposed through either a hexagonal path [33] or a tetragonal path [34]. Based on enthalpy calculations, Cai et al. [23] suggested that the phase transformation in BeO can be viewed as an orthogonal strain deformation: two strain contraction in $[10\bar{1}0]$ and $[0001]$ direction and a strain expansion in $[0100]$ direction. Alptekin and Durandurdu [26] suggested from their ab initio MD simulations that at 700 GPa the WZ BeO passed through a fivefold coordinated hexagonal intermediate state with space group $P6_3/mmc$ and a fivefold coordinated orthorhombic intermediate state with *Cmcm* symmetry and then transformed to RS phase. Correspondingly, the phase transformation occurs in two steps: initially the wurtzite structure is significantly compressed along the original [001] direction and expanded along the [100] and [010] direction (cubic simulation cell); secondly the structure is compressed along the [001], [010] and [100] directions accompanied by one angle changing from 120° to 90°. It is shown that our transformation pressure and mechanism obtained from both the LDA and GGA methods are different from the ab initio MD simulations performed by Alptekin and Durandurdu [26] who employed Siesta code and simulated the high pressure-induced phase transformation using the GGA method with Γ point sampling, a cutoff energy of 150 Ry and DZP basis set based on a cubic simulation cell consisting of 72 atoms. In our work, the pressure is applied step by step and is increased at a rate of 20 GPa, and the system is equilibrated for 2 ps at each pressure, whereas in reference [26] the equilibration period is 1000 fs for each increment and the rate of increasing pressure is not clear. The large

discrepancy in the phase transformation mechanism may be mainly caused by the difference in the way of applying pressure. It is suggested that the way of applying pressure has significant effects on the transformation pathway in ab initio MD simulations of high pressure-induced phase transformation.

Ab initio MD simulations of ZB BeO under high pressure

For ZB BeO, the simulations based on the LDA method show that the system remains the zinc blende structure up to 140 GPa, and a phase transition from the ZB to RS structure occurs when the pressure is increased to 160 GPa. Figure 7 shows the variation of the simulation cell lengths and angles with time at 160 GPa for BeO in the zinc blende phase. The simulation cell vectors **A**, **B**, and **C** in Fig. 7a are along the [100], [010], and [001] directions in the original zinc blende structure, respectively. Upon structural phase transformation, the decrease of |**C**| and increase of |**A**| and |**B**| occur simultaneously, corresponding to compression in [001] direction and expansion in [100] and [010] direction. Meanwhile, the gamma angle between the **A** and **B** lattice vectors increases significantly from 90° to ~110° (as shown in Fig. 7b), corresponding to a monoclinic adaption of the simulation cell. A rocksalt structure is observed to form at $t \approx 1.562$ ps. The schematic view of geometrical structures of BeO at 160 GPa before and after phase transformation is illustrated in Fig. 8a. The transformation pathway in zinc blende BeO is shown to be similar to ZB AlN [35], ZB GaN [32], and ZB SiC [36]. Figure 8b shows the atomic coordination of BeO at 160 GPa before and after phase transformation. Before transformation the Be_1 atom is four-coordinated to O_2, O_4, O_5, and O_6 atoms with an average ⟨Be–O⟩ bond length of 1.46 Å. The distance from Be_1 to O_1 and O_3 is 2.82 and 2.81 Å, respectively. After phase transformation, the Be_1 atom is six-coordinated to O_1, O_2, O_3, O_4, O_5, and O_6 atoms with an average bond length of 1.58 Å. Accompanied by the monoclinic deformation of the simulation cell, all the atoms shift along the [100] direction. Besides, Be_1, O_2, O_4, O_5, and O_6 atoms also shift in $[00\bar{1}]$ direction of original zinc blende structure.

Similar to the case of WZ BeO, a different mechanism is also revealed by the GGA method. The variation of the simulation cell lengths and angles with time at 120 GPa for BeO in the zinc blende phase is presented in Fig. 9. It is shown that as the phase transformation takes place, the |**A**| decreases and |**B**| and |**C**| increase. During this process, the simulation angles initially oscillate slightly and the alpha angle then goes through a decrease from 90° to ~70°. This monoclinic adaption of the simulation cell shows different

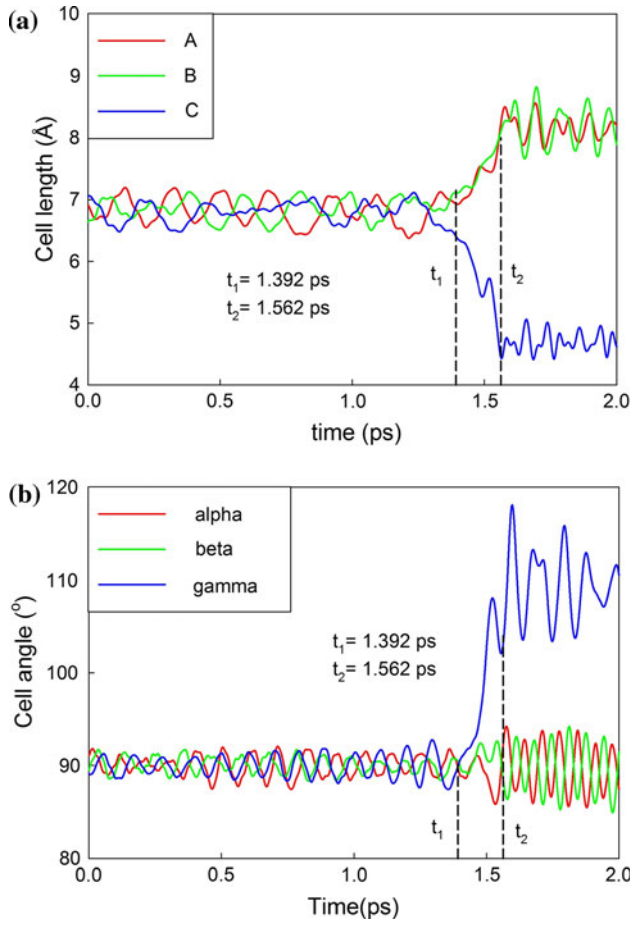

Fig. 7 Variation of the simulation cell lengths (**a**) and angles (**b**) as a function of MD time step for ZB BeO at 160 GPa obtained from the LDA method

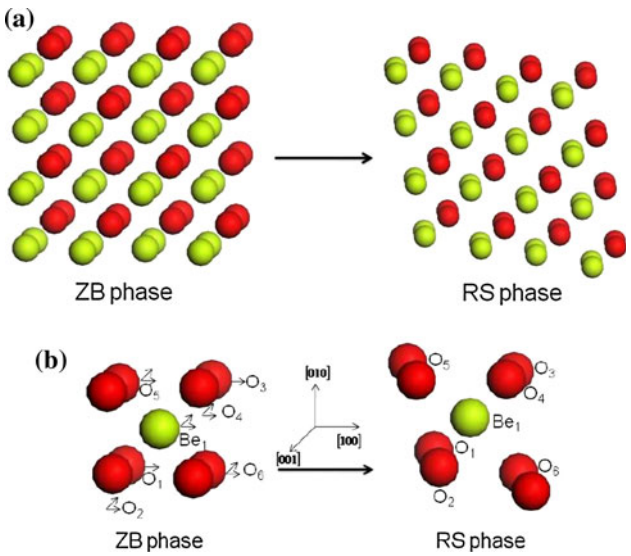

Fig. 8 Schematic view (on the (001) plane) of **a** the geometrical structure, **b** atomic coordination, **c** planar atomic structure of BeO at 160 GPa before (ZB structure) and after (RS structure) phase transformation obtained from the LDA method

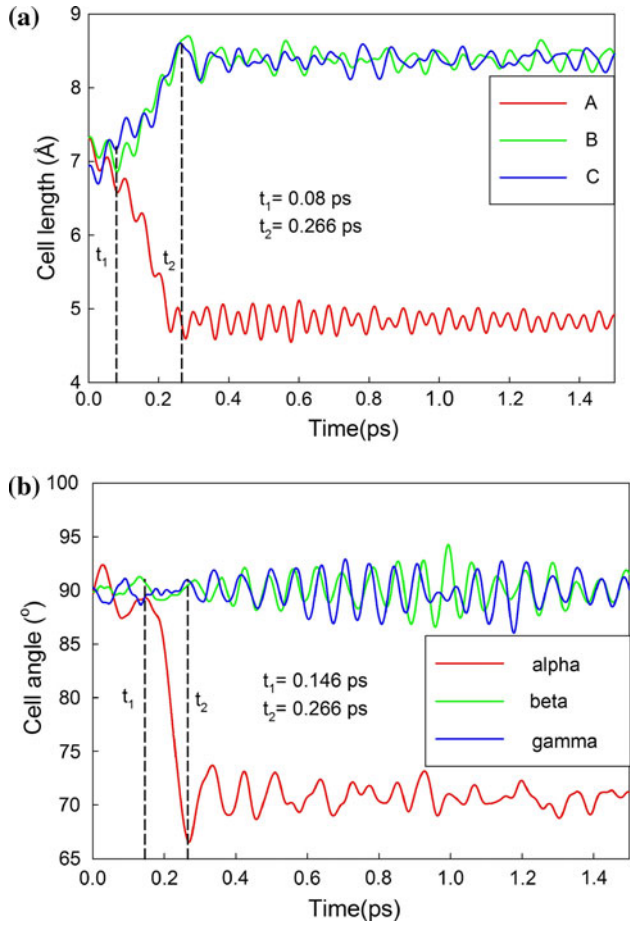

Fig. 9 Variation of the simulation cell lengths (**a**) and angles (**b**) as a function of MD time step for ZB BeO at 120 GPa obtained from the GGA method

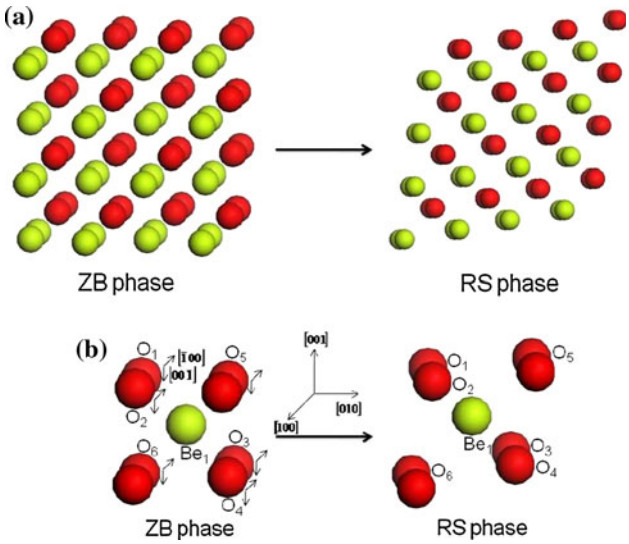

Fig. 10 Schematic view (on the (100) plane) of **a** the geometrical structure, **b** atomic coordination, **c** planar atomic structure of BeO at 120 GPa before (ZB structure) and after (RS structure) phase transformation obtained from the GGA method

character from the simulations based on the LDA method. The schematic view of geometrical structures of BeO at 120 GPa before and after phase transformation is illustrated in Fig. 10a. Figure 10b shows the atomic coordination of BeO at 120 GPa before and after phase transformation. Before transformation the bond length between Be_1 and O_1 (O_3, O_5 and O_6) is 1.52 Å and O_2 and O_4 are 2.91 Å away from the Be_1 atom. All the atoms shift in $[\bar{1}00]$ and $[00\bar{1}]$ directions with different displacements until a rocksalt structure is formed. It is shown that for both WZ → RS and ZB → RS phase transformations in BeO the transformation mechanisms revealed from the ab initio MD simulations are dependent on the exchange–correlation functional employed.

Conclusion

Ab initio MD calculations have been performed to study the phase stability of BeO under high pressure. Enthalpy calculations show that WZ → RS and ZB → RS phase transformations will occur at high pressure, and no WZ → ZB phase transformation is predicted. In our ab initio MD simulations, the WZ → RS phase transformations are observed to take place at 180 and 140 GPa by the LDA and GGA simulations, respectively. For both methods, the WZ → RS transformation proceeds smoothly without passing through ZB phase; however, different transformation pathways have been revealed. As the exchange–correlation functional is described by the LDA method, the atoms in the simulation cell mainly shift toward opposite directions: $[1\bar{2}10]$ and $[\bar{1}2\bar{1}0]$, accompanied by shift in $[10\bar{1}0]$ and $[000\bar{1}]$ directions, resulting in a phase transformation to rocksalt structure. In the case of the GGA method, the phase transformation is mainly caused by the shift of all the atoms in the $[\bar{1}2\bar{1}0]$ direction with different displacement and slight movements in $[10\bar{1}0]$ and $[000\bar{1}]$ directions. This mechanism is different from the previous ab initio MD simulations of WZ BeO at 700 GPa based on the GGA method. For pressure-induced ZB → RS phase transformation, the phase transition pressure and mechanisms also vary with the exchange–correlation functional employed. It is shown that both the exchange–correlation functional and the way of applying pressure affect the transformation pathway in ab initio MD simulations of high pressure-induced phase transformation.

Acknowledgements This work was supported by the Project Sponsored by the Scientific Research Foundation for the Returned Overseas Chinese Scholars, State Education Ministry, by the National Natural Science Foundation of China (No. 11004023), and by part of the Materials Science of Actinides, an Energy Frontier Research Center funded by the U.S. Department of Energy, Office of Science,

Office of Basic Energy Sciences under Award Number DE-SC0001089.

References

1. Slack GA, Austerman SB (1971) J Appl Phys 42(12):4713
2. Roessler DM, Walker WC, Loh E (1969) J Phys Chem Solids 30(1):157
3. Hazen RM, Finger LW (1986) J Appl Phys 59(11):3728
4. Duman S, Sütlü A, Bağcı S, Tütüncü HM, Srivastava GP (2009) J Appl Phys 105(3):033719
5. Sorokin PB, Fedorov AS, Chernozatonskiĭ LA (2006) Phys Solid State 48(2):398
6. Baumeier B, Krüger P, Pollmann J (2007) Phys Rev B 76(8):085407
7. Loh E (1968) Phys Rev 166(3):673
8. Wdowik UD (2010) J Phys 22(4):045404
9. Iwanaga H, Kunishige A, Takeuchi S (2000) J Mater Sci 35(10):2451. doi:10.1364/JOSAB.27.002026
10. Jephcoat AP, Hemley RJ, Mao HK, Cohen RE, Mehl MJ (1988) Phys Rev B 37(9):4727
11. Cline CF, Stephens DR (1965) J Appl Phys 36(9):2869
12. Cline CF, Dunegan HL, Henderson GW (1967) J Appl Phys 38(4):1944
13. Marsh SP (1973) High Temp High Press 5:503
14. Mori Y, Ikai T, Takarabe K (2003) Photon Fact Act Rep 20B:215
15. Ma Y, Skytt P, Wassdahl N, Glans P, Guo J, Nordgren J (1993) Phys Rev Lett 71(22):3725
16. Harada Y, Tokushima T, Takata Y, Takeuchi T, Kitajima Y, Tanaka S, Kayanuma Y, Shin S (2004) Phys Rev Lett 93(1):017401
17. Chang KJ, Froyen S, Cohen ML (1983) J Phys C 16(18):3475
18. Chang KJ, Cohen ML (1984) Solid State Commun 50(6):487
19. Camp PEV, Doren VEV (1996) J Phys 8(19):3385
20. Boettger JC, Wills JM (1996) Phys Rev B 54(13):8965
21. Park CJ, Lee SG, Ko YJ, Chang KJ (1999) Phys Rev B 59(21):13501
22. Milman V, Warren MC (2001) J Phys 13(2):241
23. Cai Y, Wu S, Xu R, Yu J (2006) Phys Rev B 73(18):184104
24. Amrani B, Hassan FEH, Akbarzadeh H (2007) J Phys 19(43):436216
25. Song HF, Liu HF, Tian E (2007) J Phys 19(45):456209
26. Alptekin S, Durandurdu M (2009) Solid State Commun 149(9–10):345
27. Xiao HY, Gao F, Wang LM, Zu XT, Zhang Y, Weber WJ (2008) Appl Phys Lett 92(24):241909
28. Soler JM, Artacho E, Gale JD, García A, Junquera J, Ordejón P, Sánchez-Portal D (2002) J Phys 14(11):2745
29. Troullier N, Martins JL (1991) Phys Rev B 43(3):1993
30. Parrinello M, Rahman A (1981) J Appl Phys 52(12):7182
31. Mori Y, Niiya N, Ukegawa K, Mizuno T, Takarabe K, Ruoff AL (2004) Phys Status Solidi B 241(14):3198
32. Xiao HY, Gao F, Zu XT, Weber WJ (2010) J Alloys Compd 490:537
33. Serrano J, Rubio A, Hernández E, Muñoz A, Mujica A (2000) Phys Rev B 62:16612
34. Knudson MD, Gupta YM, Kunz AB (1999) Phys Rev B 59:11704
35. Durandurdu M (2008) J Phys Chem Solids 69:2894
36. Shimojo F, Ebbsjö I, Kalia RK, Nakano A, Rino JP, Vashishta P (2000) Phys Rev Lett 84:3338